ACS APPLIED MATERIALS & INTERFACES

Research Article

www.acsami.org

Controlled Directional Crystallization of Oligothiophenes Using Zone Annealing of Preseeded Thin Films

Changhuai Ye,[†] Lei Zhang,[‡] Guopeng Fu,[†] Alamgir Karim,[†] Thein Kyu,[†] Alejandro L. Briseno,[‡] and Bryan D. Vogt*[,†]

[†]Department of Polymer Engineering, University of Akron, Akron, Ohio 44325, United States

[‡]Department of Polymer Science & Engineering, University of Massachusetts, Amherst, Massachusetts 01003, United States

Supporting Information

ABSTRACT: We demonstrate a simple route to directionally grow crystals of oligothiophenes, based on 2,5-bis(3-alkylthiophen-2-yl)thieno[3,2-*b*]thiophene with degrees of polymerization of 2 (BTTT-2) and 4 (BTTT-4) via zone annealing (ZA) of preseeded films. ZA of spun-cast films of BTTT-2 does not yield highly aligned crystals. However, if the film is oven-annealed briefly prior to ZA, highly aligned crystals that are millimeters in length can be grown, whose length depends on the velocity of the ZA front. The precrystallized region provides existing nuclei that promote crystal growth and limit nucleation of new crystals in the melted region. Aligned crystals of BTTT-2 can be obtained even when the moving velocity for ZA is an order of magnitude greater than the crystal growth rate. The relative nucleation rate to the crystallization rate for BTTT-4 is greater than that for BTTT-2, which decreases the length over which BTTT-4 can be aligned to ~500 μm for the conditions examined. The temperature gradient and moving velocity of ZA enable control of the length of the aligned crystalline structure at the macroscale.

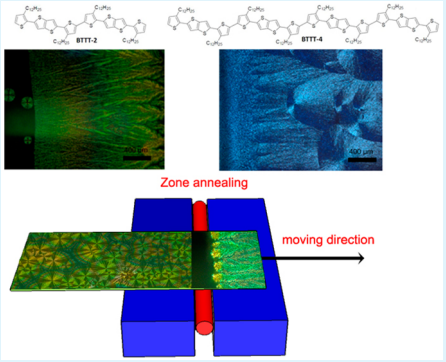

KEYWORDS: *directed crystallization, thermal gradient, organic electronics, P3HT, pentacene*

1. INTRODUCTION

Organic electronics holds tremendous promise for large-area and low-cost devices,[1] but the performances of organic semiconductors are generally inferior to their inorganic counterparts because of their semicrystalline structure, which is processing-dependent.[2,3] In particular, grain boundaries are believed to be bottlenecks to charge transport in organic thin-film transistors (OTFTs).[4] Thus, larger crystal grains with fewer grain boundaries are preferred,[5,6] but it is, in general, difficult to grow large crystals in a simple and manufacturable process. Aligned and directional crystal growth of organic semiconductors significantly enhances the grain size and performance of OTFTs.[7,8] A variety of methods based on solution processing enable controlled crystallization, such as epitaxial crystallization,[9] flow coating,[10] dip coating,[11] nucleation additives,[6] and zone casting.[7,12] However, not all of these strategies can be readily scaled-up for production, and thus scalable, alternative postcasting strategies for improving the performance of organic electronic devices have also been explored.[2] For example, exposure of the semiconductor film to solvent vapor can provide sufficient molecular mobility to enhance the crystallinity and transistor performance.[13] Alternatively, the substrate chemistry can be modified to promote crystallization.[14] However, these methods still tend to lead to grain-boundary-rich polycrystalline films, which likely limits the performance.[15]

Historically, the growth of single-crystal ingots through zone annealing (ZA; melting) was used to refine the metals and inorganic materials by localized and directional melting and recrystallization.[16] In the 1960s and 1970s, this technique was extended to grow large crystals of polyolefins[17] and poly(ethylene oxide).[18,19] The alignment of the crystalline structure is controlled by the crystal growth rate, the temperature gradient, and the moving velocity of ZA.[18] Subsequently, in the past decade, ZA has been extended for the alignment of microdomains of block copolymers,[20] including thin films.[21] This alignment of the liquid-crystalline order in block copolymers leads to anisotropic properties.[22] Similarly, ZA has been utilized to increase the crystallinity of optoelectronic small molecules in thin films, which tends to enhance their properties,[23] but this has not typically generated highly aligned single crystals. ZA methods have been extended to organic semiconductors to grow bulk ingots of single crystals.[24] This technique has been used sporadically for organic electronics in thin films,[23,25] but few reports have fundamentally examined the underlying physics associated with the growth of aligned crystals. Geerts and co-workers elegantly described the ability to use temperature gradients to induce different polymorphs in terthiophene, but these films tend to also include cracks as the

Received: July 14, 2015
Accepted: September 28, 2015
Published: September 28, 2015

DOI: 10.1021/acsami.5b06344
ACS Appl. Mater. Interfaces 2015, 7, 23008−23014

Scheme 1. Molecular Structures of BTTT-2 and BTTT-4

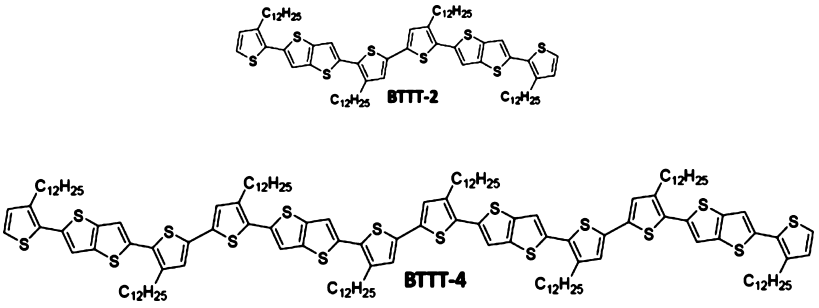

uniaxially oriented films are cooled to room temperature.[26] It is still unclear how to best select processing conditions for a given organic semiconductor and whether ZA is applicable to all families of crystalline organic semiconductors.

Here we illustrate how to extend ZA to highly crystalline oligothiophenes.[27,28] In particular, we will examine 2,5-bis(3-alkylthiophen-2-yl)thieno[3,2-*b*]thiophene (BTTT)[29] with degrees of polymerization of 2 (BTTT-2) and 4 (BTTT-4). BTTT-4 exhibits a modest device performance with a mobility between 0.002 and 0.01 $cm^2\ V^{-1}\ s^{-1}$ in thin-film transistors. However, BTTT-2 exhibits a mobility of only $10^{-4}\ cm^2\ V^{-1}\ s^{-1}$ because of the crossed stacks in its crystal packing.[29] Thus, the crystal structure of BTTT-2 adversely impacts the performance, and potential control of its crystal structure (orientation and polymorph) through ZA could prove advantageous. A sharp temperature gradient was used to directionally grow the BTTT crystalline structure. The morphology depends on the initial crystal state of the film, the temperature gradient, and the moving velocity of ZA. With seeded growth, oriented crystals of BTTT are obtained even when the velocity of ZA exceeds the isothermal crystal growth rate by nearly an order of magnitude. Isothermal crystallization kinetics provides guidelines for the selection of processing parameters to produce directional crystallization.

2. EXPERIMENTAL SECTION

Materials. Toluene (>99.5%, ACS reagent) was purchased from Sigma-Aldrich. Sulfuric acid (>51% H_2SO_4) was purchased from Avantor Performance Materials, Inc. Hydrogen peroxide (H_2O_2, 30% aqueous solution) was purchased from EMD Chemicals Inc. All of the materials were used as received. Poly(dimethylsiloxane) (PDMS; Sylgard 184, Dow Corning) was prepared by mixing the base and curing agent in a mass ratio of 5:1 and subsequently curing at ambient temperature for 4 h, followed by 120 °C for 2 h. The synthesis and purification of BTTT-2 and BTTT-4 were reported previously.[29] The molecular structures of BTTT-2 and BTTT-4 are shown in Scheme 1. Table 1 provides the key characteristics of the two oligothiophenes.

Table 1. Characteristics of BTTT-2 and BTTT-4[a]

	M_n (g mol^{-1})	T_m (°C)	T_c (°C)	ΔH_m (J g^{-1})
BTTT-2	1280	101	32	35.6
BTTT-4	2558	116	66	33.6

[a]Determined from differential scanning calorimetry at 10 °C min^{-1}.

Sample Preparation. A 1 wt % BTTT solution was prepared by dissolving BTTT in toluene. Quartz substrates (75 mm × 25 mm × 0.65 mm; GM Associates) were cleaned using piranha solution (H_2SO_4:H_2O_2 (30 wt %) = 70:30) at 90 °C for 30 min, followed by rinsing using deionized water several times. Approximately 40−50 μL of a BTTT solution was drop-cast onto the quartz substrate and spread over an area of approximately 2 cm × 2 cm. The dried film was approximately 1 μm thick. PDMS with a thickness of approximately 0.3 mm was cut into the same size as quartz-supported BTTT films. PDMS was placed on top of the BTTT film to minimize flow of the BTTT melt during the ZA process.

Isothermal Crystallization. BTTT-2 films were isothermally crystallized on a temperature-controlled hot stage (TMS 93, Linkam). The heated films were imaged with a polarized optical microscope (BX60, Olympus). The supported BTTT-2 were first heated to 110 °C for 10 min and then quenched at 20 °C min^{-1} to the desired isothermal crystallization temperature. BTTT-4 films were heated to 130 °C for approximately 10 min and then quenched to the desired temperature for isothermal crystallization. The crystallization was tracked in situ by microscopy to determine the crystallization rate. Images were recorded every 60 s to elucidate the temporal evolution of the spherulites during crystallization.

Crystallization Using ZA. ZA-induced directional crystallization of BTTT-2 and BTTT-4 films. The ZA set-up was previously described in detail.[30] Briefly, a heating filament between two cold blocks was used to generate a sharp temperature gradient on the substrate with maximum temperatures of 110 °C for BTTT-2 and 130 °C for BTTT-4 (measured by a Testo 875-1 IR camera). The temperature of the cold blocks was varied to tune the sharpness of the temperature gradient and to modulate the crystallization temperature. Prior to ZA, PDMS was placed on top of the quartz-supported BTTT-2 and BTTT-4 films to confine the system. The PDMS-capped BTTT-2 and BTTT-4 films supported on quartz were translated through the hot zone at a fixed rate. After ZA, the samples were imaged with a polarized optical microscope (Olympus MX51 using an Olympus U-PO3 polarizer slider) and atomic force microscopy (AFM; Dimension Icon, Veeco Instruments Inc.). The crystal structure of select films was also examined using grazing-incidence X-ray diffraction (GIXD) at the X9 Beamline of the National Synchrotron Light Source at Brookhaven National Laboratory (BNL). An incident energy of 13.5 eV was used, and the diffraction profiles were collected on a charge-coupled-device wide-angle X-ray scattering detector.

3. RESULTS AND DISCUSSION

Figure 1 illustrates how the morphology of BTTT-2 depends on the crystallization process with a common cold temperature of 37 °C. Isothermal crystallization of the BTTT-2 film at 37 °C after melting at 110 °C yields many small spherulites, as shown in Figure 1A. The nuclei density is approximately 2300 mm^{-2}, as estimated from the polarized optical micrographs. The structure of these crystals in BTTT-2 is shown by AFM in Figure 1B. ZA of the as-cast BTTT-2 film at 0.2 μm s^{-1} with a cold block temperature of 37 °C results in an increased size of the spherulites (Figure 1C) in comparison to those derived from isothermal crystallization, but these crystals do not show any directional alignment. The nuclei density is approximately 1200 mm^{-2}. The fibril microstructure of these crystals appears to coarsen with ZA, as shown in Figure 1D. If the same ZA conditions are applied to the precrystallized films (Figure 1A),

DOI: 10.1021/acsami.5b06344
ACS Appl. Mater. Interfaces 2015, 7, 23008−23014

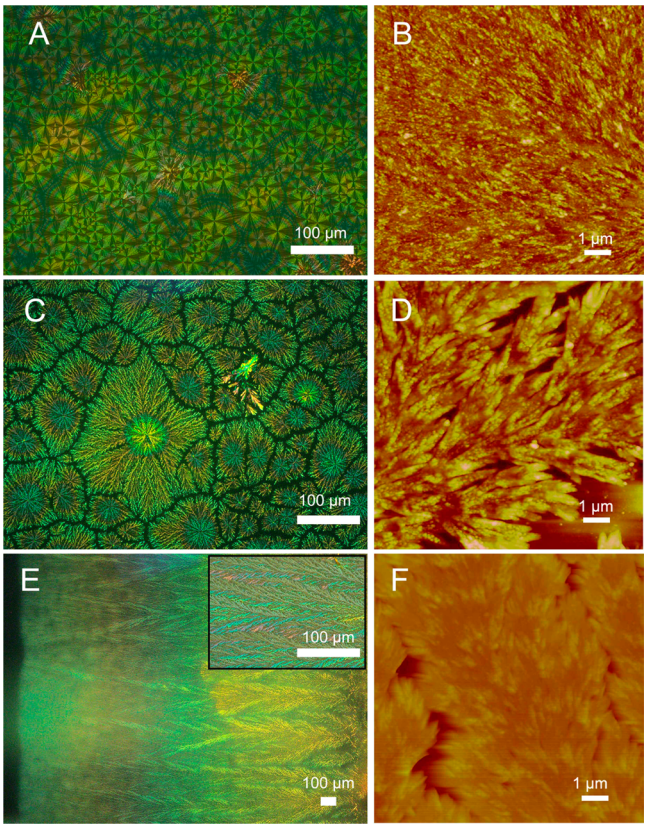

Figure 1. Crystal morphology of BTTT-2 films characterized using polarized optical microscopy and AFM after (A and B) isothermal crystallization at 37 °C, (C and D) ZA of the as-cast film, and (E and F) ZA from the precrystallized region. For the ZA processes, the moving velocity through the hot zone is 0.2 μm s^{-1}, the maximum temperature is 110 °C, and the cold block temperature is 37 °C for both cases.

the existing crystals act as nuclei for directional crystal growth. A highly aligned crystalline structure that extends millimeters is obtained from this processing (Figure 1E). However, past several millimeters, the structure reverts to random spherulites for ZA of the precrystallized film at 0.2 μm s^{-1} with a cold block temperature of 37 °C. The BTTT-2 molecules, however, are not unidirectionally aligned, as illustrated in Figure 1F; a herringbone-like morphology is evident in the AFM micrographs. In terms of the crystalline morphology of BTTT-2 films processed by different annealing conditions, isothermal crystallization leads to regular spherulite morphology. However, ZA changes the crystalline morphology to dense lamellar branching morphology.[31] ZA of preseeded BTTT-2 thin films leads to irregular side branching and tip splitting, which is normally called seaweed morphology.[32]

In order to address the differences in the morphology between parts C and E of Figure 1, the ZA process needs to be examined carefully. First, the maximum temperature of the temperature gradient at the substrate must be greater than the melting point of BTTT-2 to ensure that the crystals are locally melted. The temperature gradient also promotes natural convection in the BTTT-2 oligomers due to the low viscosity of the melt; this leads to very nonuniform film thicknesses (Figure S1). To avoid this flow (and the potential for competition between shear[33] and temperature gradient in aligning crystals), a thin (300 μm), cross-linked PDMS sheet is placed on top of the BTTT-2 film, which limits flow (see the schematic in Figure 2). The key to alignment with ZA is to fully suppress the nucleation of new crystals to allow only growth to occur once a crystal is nucleated.

For an effective directional crystal growth process by ZA, there are two primary criteria that have been established: (1) the crystal growth rate G_c at the crystallization temperature T_c must be equal to the ZA velocity and (2) no new nuclei should be formed when cooling from the melting point, T_m to T_c.[18] Typically, failure to abide by these rules leads to interruption of the directional crystal growth by new spherulites. In general, this means that the nucleation rate should be slow compared to G_c. Homogeneous nucleation is generally not significant when the undercooling is less than 50−70 °C,[34] but heterogeneous nucleation dominates in most crystallizing systems and occurs at much lower undercooling. The total number of primary

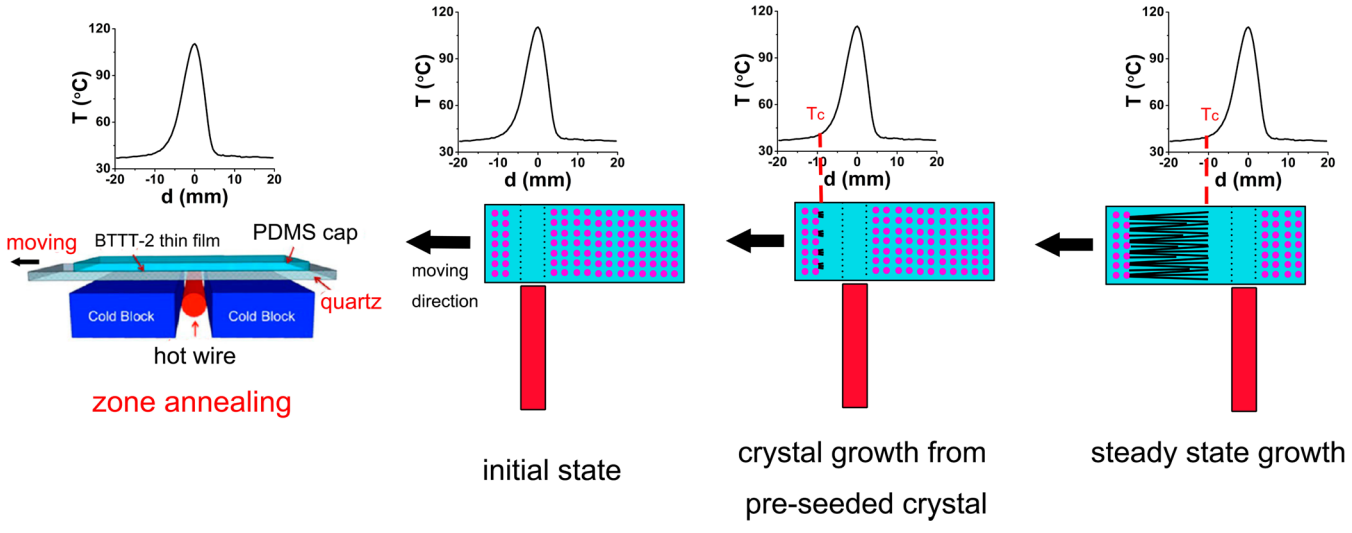

Figure 2. Schematic illustrating the ZA process for the alignment of BTTT crystallites using a preseeded approach. Initially, the precrystallized BTTT film is locally melted because of the hot zone. As the sample moves across the heating zone, the boundary between the melt and crystals moves to progressively lower temperatures. The crystals grow from this boundary as the unmelted crystals act as nuclei. The crystals directionally grow over macroscopic dimensions at T_c, where the moving velocity and crystal growth rate are equal.

DOI: 10.1021/acsami.5b06344
ACS Appl. Mater. Interfaces 2015, 7, 23008−23014

nuclei n formed when the films with a cross-sectional area A move from T_m to T_c at a velocity v is[18]

$$n = A\frac{T_c - T_m}{G_c v^2}\int_{T_m}^{T_c} N\,dT \quad (1)$$

where N is the homogeneous nucleation rate. The sharp temperature gradient for ZA suppresses the generation of nuclei, which is the key to controlling the directional growth of the crystalline structure.

The nucleation rate increases as the temperature decreases. However, for the gradient applied with ZA, the nucleation rate is zero above the melting point, so there should be a boundary in the temperature profile above which nucleation is suppressed (the total number of primary nuclei formed is 1). Assuming that this boundary is at $T = T_c$, this provides a cutoff for the maximum moving velocity for ZA. If this moving velocity is larger than the crystal growth rate at T_c, lower temperatures will be experienced by the melt, where the probability of forming new nuclei is greater than 1. In this regime, new nuclei will form as the heating zone moves, leading to a polycrystalline structure with spherulites, which is consistent with the morphology shown in Figure 1C. The larger crystal size can be rationalizede by the process history where crystallization will occur at a temperature greater than that of the cold block (37 °C); this will decrease the nucleation rate. Even by changing the ZA velocity and the temperature gradient, directionally grown crystals of BTTT-2 could not be obtained from the as-cast films because of the lower velocity limit (0.1 μm s^{-1}) for the ZA apparatus, which does not enable suppression of the nucleation.

Because the crystallization of BTTT-2 is slow and the time required to nucleate a crystal is problematic for accessible ZA velocities, we used a preseeded methodology. BTTT-2 is initially crystallized isothermally to provide existing nuclei to promote directional crystal growth, as shown schematically in Figure 2. By not melting all of the existing crystals, aligned crystal growth can be realized as the boundary between the precrystallized region and the hot melting zone, providing nuclei for crystal growth. As the hot zone moves, the crystal will preferentially grow from these existing nuclei to overcome the time constant associated with the formation of new nuclei at small undercooling. The crystal growth propagates from the original melting boundary. If the moving velocity is equal to G_c, the crystal will directionally grow from the seeded crystals. However, when the moving velocity is larger, it is expected that the directional growth of the crystal will cease. Intriguingly, we observe initially that the seeded directional growth dominates, but at some distance that nucleation of new crystals occurs to produce spherulite morphology (Figure 1E).

The crystal growth rate and nucleation rate are critical to understanding the conditions where the directional alignment would be expected from ZA based on prior investigations for polymers.[18] The crystal growth rate can be determined from isothermal crystallization. However, the nucleation rate from T_m to T_c is difficult to quantify. In order to qualitatively show how the nucleation rate changes with the temperature and relate it to the directional alignment of the crystalline structure of BTTT using ZA, the isothermally annealed BTTT melt is cooled at 1 °C min^{-1} and the nucleation is observed using polarized optical microscopy, as shown in Figure S2. BTTT-2 does not show any obvious nuclei until the temperature decreases to about 41 °C. Then the number of nuclei increases rapidly in several minutes (several degrees). BTTT-4 seems to nucleate much faster compared to BTTT-2. For BTTT-4, the nuclei first appear at 75 °C, and then the number of nuclei increases extremely fast. The nuclei completely cover the observed region in approximately 5 min. These qualitative nucleation data suggest that the directional growth of the crystal should occur at temperatures greater than 41 °C for BTTT-2 and 75 °C for BTTT-4 to minimize nucleation. Generally, the crystal growth rate must be equal to or greater than the moving velocity in ZA to obtain a directional crystalline structure. Figure 3 illustrates the growth rates G for

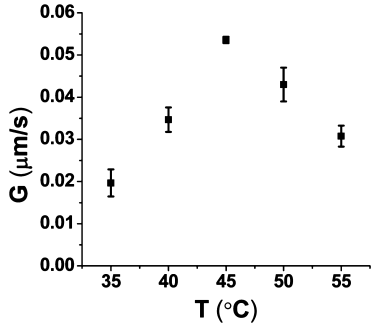

Figure 3. Isothermal crystal growth rate of BTTT-2 films under quiescent (isothermal) conditions.

spherulites of BTTT-2 under isothermal crystallization conditions. Because the undercooling is the driving force for crystallization, increasing the degree of undercooling will enhance the crystal growth rate if growth is thermodynamically controlled. However, decreasing the temperature increases the viscosity of BTTT-2. At sufficiently low temperature, the crystallization is kinetically limited by the material mobility. The competition of these two effects leads to a maximum crystal growth rate. Figure 3 shows that this maximum in G is near 45 °C, but the maximum isothermal crystal growth rate is <0.06 μm s^{-1} at all temperatures examined. Near the isothermal crystallization temperature examined previously (37 °C), the crystal growth rate is only 0.016 μm s^{-1} at 35 °C. This is more than 1 order of magnitude slower than the moving velocity for ZA previously illustrated, so it is surprising that any directional crystallization is observed. This significant difference in the rates for the standard ZA (Figure 1C) is likely responsible for the lack of directional crystallization. It is unclear how highly directional crystallization over macroscopic scales (millimeters) can be accomplished with this large discrepancy when preseeded crystals are present (Figure 1E).

In order to better understand the fundamental physics underlying this directed crystallization, the temperature profile during ZA was systematically varied by changing the temperature of the cold blocks, while maintaining a constant maximum temperature at approximately T_m + 10 °C. At a fixed moving velocity of 0.5 μm s^{-1}, which is about 10 times higher than the maximum crystal growth rate of BTTT-2, some directional crystallization is observed in all cases for the preseed (annealed) films, as shown in Figure 4. At the lowest temperature examined (25 °C, Figure 4A), the length of the aligned crystalline structure is only 173 μm, after which the film reverts to spherulites. A similar behavior is observed as the cold block temperature is increased, but the length of the aligned crystalline region increases to 368 μm (Figure 4B), 885 μm (Figure 4C), and 1421 μm for 32, 37, and 42 °C, respectively.

DOI: 10.1021/acsami.5b06344
ACS Appl. Mater. Interfaces 2015, 7, 23008−23014

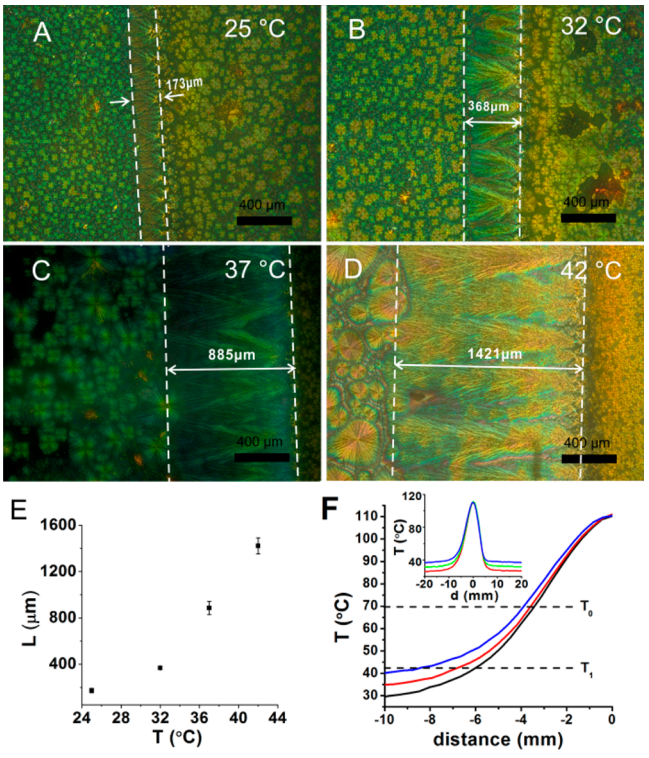

Figure 4. Polarized optical micrographs of BTTT-2 films after ZA with a moving velocity of 0.5 μm s^{-1} and cold block temperatures of (A) 25, (B) 32, (C) 37, and (D) 42 °C. (E) Effect of the cold block temperature on the aligned length of the crystalline structure of BTTT-2 films. (F) Temperature profiles of ZA for BTTT-2 films at various cold block temperatures examined.

Figure 4E illustrates how the length of the aligned crystal, l_c, depends on the cold block temperature. To understand this cold block temperature effect, the temperature gradient for each condition is shown in Figure 4F. As the moving velocity is 0.5 μm s^{-1}, which is much faster than even the maximum crystal growth rate at ~45 °C, the crystals likely grow directionally at temperatures higher than 41 °C, where crystal growth dominates, as shown in Figure S2. We can consider that the directional crystal growth occurs between the region T_0 and T_1, where the nucleation rate is relatively small compared to the growing rate. Then the length of the aligned crystal is dependent on the distance between T_0 and T_1, which is dependent on the broadness of the temperature gradient in ZA. The temperature gradient becomes sharper as the cold block temperature is decreased. Assuming that T_0 = 70 °C and T_1 = 42 °C, the lengths between T_0 and T_1 are 4.6, 3.2, and 2.6 mm as the cold block temperature decreases, as shown in Figure 4F. The temperature gradient from T_0 to T_1 is not constant, and the crystal growth rate has a maximum at around 45 °C, so the aligned crystal length would be expected to be proportional to the length between T_0 and T_1 (consistent with the experimental results). However, the sharper temperature gradient should be more effective at preventing nucleation (eq 1). Thus, T_1 for higher cold block temperature is actually slightly higher than that for lower cold block temperature. Nonetheless, the broad temperature gradient is effective for the directional growth of the crystal in the cases examined.

To further investigate the role of processing parameters on the efficacy of ZA of the slow crystallizing BTTT-2, the influence of the moving velocity is examined for a fixed cold block temperature of 37 °C. In this case, the velocity still exceeds the maximum G determined from isothermal crystallization (Figure 2). This provides a route to probe how l_c scales with the departure from the maximum isothermal crystallization rate. As the moving velocity increases, the time for the melt to reach the position at T_c decreases. As a result, the length of the aligned crystal becomes shorter, which can be clearly seen from polarized optical images, as shown in Figure 5A–D. The aligned length of the crystal is only 324 μm when

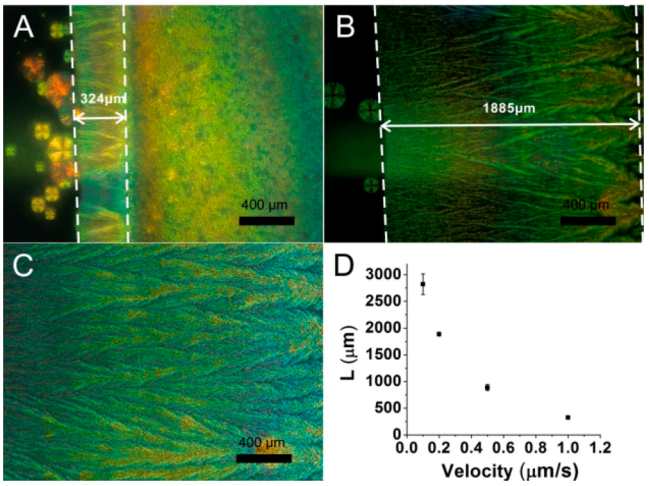

Figure 5. Polarized optical micrographs of BTTT-2 films after ZA at a constant cold block temperature of 37 °C with different moving velocities of (A) 1, (B) 0.2, and (C) 0.1 μm s^{-1}. (D) Length of the aligned crystal by ZA with varied moving velocities.

the moving velocity is 1 μm s^{-1}. As the moving velocity decreases to 0.5 and 0.2 μm s^{-1}, the aligned length increases to 885 and 1885 μm. Upon further lowering of the moving velocity to 0.1 μm s^{-1}, the aligned length increases to approximately 2.8 mm. This moving velocity is a factor of 2 greater than the maximum isothermal crystallization rate for BTTT-2, so this preseeded approach appears to enable large-scale growth of directional crystals.

The principles of the directed crystallization of the BTTT-2 film using ZA can be applied in the BTTT-4 film, which has a similar crystal growth rate but a much larger nucleation rate at the same supercooling. Isothermal crystallization of the BTTT-4 film at 70 °C shows the expected spherulitic polycrystalline structure, as shown in Figure 6A. The nuclei density for BTTT-4 isothermal crystallization at 70 °C (46 °C of undercooling) is approximately 2786 mm^{-2}, which is larger than that for BTTT-2 crystallized at 37 °C (64 °C of undercooling). This result suggests that the intrinsic crystal growth rate for BTTT-4 is significantly less than that for BTTT-2. Using preseeded ZA at a moving velocity of 0.1 μm s^{-1} and with a maximum temperature of 130 °C and a cold block temperature of 35 °C, a small length of the directional crystalline structure can be formed at the beginning of the ZA process for BTTT-4. However, the crystalline structure transforms to spherulites at a relatively short distance, but qualitatively this behavior is similar to ZA for BTTT-2 films. Because the nucleation rate for BTTT-4 is much faster than that for BTTT-2 at the same supercooling, the time for directional crystal growth of BTTT-4 is shorter than that of BTTT-2 under similar ZA conditions (see Figure 6B). When the cold block temperature is increased to 70 °C, the length of the aligned crystal increases.

DOI: 10.1021/acsami.5b06344
ACS Appl. Mater. Interfaces 2015, 7, 23008–23014

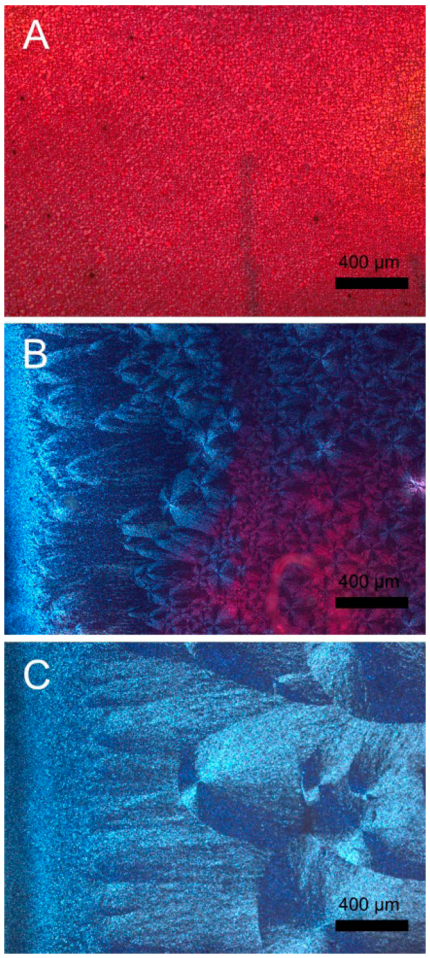

Figure 6. (A) BTTT-4 film isothermal crystallization at 70 °C. BTTT-4 films using preseeded ZA at cold block temperatures of (B) 35 and (C) 70 °C. The moving velocity for ZA is 0.1 μm s^{-1}, and the maximum temperature is set as 130 °C.

Furthermore, although the directional crystal growth is interrupted by newly formed nuclei, large and asymmetric spherulites are obtained after the aligned crystalline structure because of the suppressed nucleation by the temperature gradient and relative high cold block temperature (Figure 6C). This methodology provides a simple route to relatively large crystals with directional growth and is likely extendable to other conjugated crystalline materials.

4. CONCLUSIONS

ZA was used to align the crystalline structures of the BTTT-2 and BTTT-4 thin films. Although the crystal growth rate is low, as determined by isothermal crystallization with a maximum crystal growth rate of <0.06 μm s^{-1}, aligned crystals can be formed by ZA at significantly larger velocities by using existing crystals as preseeded nuclei. Increasing the cold block temperature for ZA increases the length of the aligned crystalline structure because of the breadth of the gradient, which is counter to standard ZA, where a sharper gradient is favored. Reducing the moving velocity of ZA also increases the length of the aligned crystalline structure to improve performance in organic electronics. The crystalline structure of BTTT-2 can be aligned over millimeters at a moving velocity of 0.1 μm s^{-1}, which was still almost twice of the maximum crystal growth rate for BTTT-2. This preseeded ZA method is likely applicable to other organic semiconductors for the alignment of the crystalline structure.

■ ASSOCIATED CONTENT

Supporting Information

The Supporting Information is available free of charge on the ACS Publications website at DOI: 10.1021/acsami.5b06344.

Polarized optical micrographs of BTTT-2 and BTTT-4 under transient crystallization, time-resolved optical micrographs for isothermal crystallization, GIXD profiles, and a crystal growth curve (PDF)

■ AUTHOR INFORMATION

Corresponding Author

*E-mail: vogt@uakron.edu.

Notes

The authors declare no competing financial interest.

■ ACKNOWLEDGMENTS

A.K. acknowledges funding from the National Science Foundation (Grant NSF-DMR 1411046) for the ZA aspects of the work. L.Z. and A.L.B. thank the Office of Naval Research for support of this work (Grant N0001471410053). C.Y. thanks Kevin Yager (BNL) for assistance with the GIXD experiments. Research was carried out, in part, at the Center for Functional Nanomaterials, BNL, which is supported by the U.S. Department of Energy, Office of Basic Energy Science (Contract No. DE-SC0012704).

■ REFERENCES

(1) Dimitrakopoulos, C. D.; Malenfant, P. R. L. Organic Thin Film Transistors for Large Area Electronics. *Adv. Mater.* **2002**, *14*, 99−117.
(2) Hiszpanski, A. M.; Loo, Y. L. Directing the Film Structure of Organic Semiconductors via Post-Deposition Processing for Transistor and Solar Cell Applications. *Energy Environ. Sci.* **2014**, *7*, 592−608.
(3) Rigas, G. P.; Shkunov, M. Solution Processable Semiconducting Organic Single Crystals. *Polym. Sci., Ser. C* **2014**, *56*, 20−31.
(4) Lee, S. S.; Mativetsky, J. M.; Loth, M. A.; Anthony, J. E.; Loo, Y. L. Quantifying Resistances across Nanoscale Low- and High-Angle Interspherulite Boundaries in Solution-Processed Organic Semiconductor Thin Films. *ACS Nano* **2012**, *6*, 9879−9886.
(5) McCulloch, I.; Heeney, M.; Bailey, C.; Genevicius, K.; Macdonald, I.; Shkunov, M.; Sparrowe, D.; Tierney, S.; Wagner, R.; Zhang, W. M.; Chabinyc, M. L.; Kline, R. J.; McGehee, M. D.; Toney, M. F. Liquid-Crystalline Semiconducting Polymers with High Charge-Carrier Mobility. *Nat. Mater.* **2006**, *5*, 328−333.
(6) Lee, S. S.; Kim, C. S.; Gomez, E. D.; Purushothaman, B.; Toney, M. F.; Wang, C.; Hexemer, A.; Anthony, J. E.; Loo, Y. L. Controlling Nucleation and Crystallization in Solution-Processed Organic Semiconductors for Thin-Film Transistors. *Adv. Mater.* **2009**, *21*, 3605−3609.
(7) Duffy, C. M.; Andreasen, J. W.; Breiby, D. W.; Nielsen, M. M.; Ando, M.; Minakata, T.; Sirringhaus, H. High-Mobility Aligned Pentacene Films Grown by Zone-Casting. *Chem. Mater.* **2008**, *20*, 7252−7259.
(8) Yuan, Y. B.; Giri, G.; Ayzner, A. L.; Zoombelt, A. P.; Mannsfeld, S. C. B.; Chen, J. H.; Nordlund, D.; Toney, M. F.; Huang, J. S.; Bao, Z. Ultra-High Mobility Transparent Organic Thin Film Transistors Grown by an Off-Centre Spin-Coating Method. *Nat. Commun.* **2014**, *5*, 3005.
(9) Zhou, H. X.; Jiang, S. D.; Yan, S. K. Epitaxial Crystallization of Poly(3-hexylthiophene) on a Highly Oriented Polyethylene Thin Film from Solution. *J. Phys. Chem. B* **2011**, *115*, 13449−13454.
(10) Sakamoto, K.; Ueno, J.; Bulgarevich, K.; Miki, K. Anisotropic Charge Transport and Contact Resistance of 6,13-Bis-

DOI: 10.1021/acsami.5b06344
ACS Appl. Mater. Interfaces 2015, 7, 23008−23014

(Triisopropylsilylethynyl) Pentacene Field-Effect Transistors Fabricated by a Modified Flow-Coating Method. *Appl. Phys. Lett.* **2012**, *100*, 123301.
(11) Sele, C. W.; Kjellander, B. K. C.; Niesen, B.; Thornton, M. J.; van der Putten, J. B. P. H.; Myny, K.; Wondergem, H. J.; Moser, A.; Resel, R.; van Breemen, A. J. J. M.; van Aerle, N.; Heremans, P.; Anthony, J. E.; Gelinck, G. H. Controlled Deposition of Highly Ordered Soluble Acene Thin Films: Effect of Morphology and Crystal Orientation on Transistor Performance. *Adv. Mater.* **2009**, *21*, 4926−4931.
(12) Su, Y.; Gao, X.; Liu, J.; Xing, R.; Han, Y. Uniaxial Alignment of Triisopropylsilylethynyl Pentacene via Zone-Casting Technique. *Phys. Chem. Chem. Phys.* **2013**, *15*, 14396−14404.
(13) Dickey, K. C.; Anthony, J. E.; Loo, Y. L. Improving Organic Thin-Film Transistor Performance through Solvent-Vapor Annealing of Solution-Processable Triethylsilylethynyl Anthradithiophene. *Adv. Mater.* **2006**, *18*, 1721−1726.
(14) Gundlach, D. J.; Royer, J. E.; Park, S. K.; Subramanian, S.; Jurchescu, O. D.; Hamadani, B. H.; Moad, A. J.; Kline, R. J.; Teague, L. C.; Kirillov, O.; Richter, C. A.; Kushmerick, J. G.; Richter, L. J.; Parkin, S. R.; Jackson, T. N.; Anthony, J. E. Contact-Induced Crystallinity for High-Performance Soluble Acene-Based Transistors and Circuits. *Nat. Mater.* **2008**, *7*, 216−221.
(15) Dong, H. L.; Fu, X. L.; Liu, J.; Wang, Z. R.; Hu, W. P. 25th Anniversary Article: Key Points for High-Mobility Organic Field-Effect Transistors. *Adv. Mater.* **2013**, *25*, 6158−6182.
(16) Pfann, W. G. Zone Melting: This Technique Offers Unique Advantages in Purification and in Control of Composition in Various Substances. *Science* **1962**, *135*, 1101−1109.
(17) Sasaguri, K.; Yamada, R.; Stein, R. S. Relationship between Morphology and Deformation Mechanisms of Polyolefins. *J. Appl. Phys.* **1964**, *35*, 3188−3194. Lovinger, A. J.; Chua, J. O.; Gryte, C. C. Studies on the alpha and beta Forms of Isotactic Polyproylene by Crystallization in a Temperature Gradient. *J. Polym. Sci., Polym. Phys. Ed.* **1977**, *15*, 641−656.
(18) Lovinger, A. J.; Gryte, C. C. Morphology of Directionally Solidified Poly(Ethylene Oxide) Spherulites. *Macromolecules* **1976**, *9*, 247−253.
(19) Hansen, D.; Taskar, A. N.; Casale, O. Method for Studying Polymer Crystallization in a Temperature-Gradient Field with Controlled Crystal-Growth. *J. Polym. Sci., Polym. Phys. Ed.* **1972**, *10*, 1615−1619.
(20) Mita, K.; Tanaka, H.; Saijo, K.; Takenaka, M.; Hashimoto, T. Cylindrical Domains of Block Copolymers Developed via Ordering under Moving Temperature Gradient. *Macromolecules* **2007**, *40*, 5923−5933.
(21) Berry, B. C.; Bosse, A. W.; Douglas, J. F.; Jones, R. L.; Karim, A. Orientational Order in Block Copolymer Films Zone Annealed below the Order-Disorder Transition Temperature. *Nano Lett.* **2007**, *7*, 2789−2794.
(22) Ye, C. H.; Singh, G.; Wadley, M. L.; Karim, A.; Cavicchi, K. A.; Vogt, B. D. Anisotropic Mechanical Properties of Aligned Polystyrene-block-polydimethylsiloxane Thin Films. *Macromolecules* **2013**, *46*, 8608−8615.
(23) Liu, C. Y.; Bard, A. J. Increased Photo- and Electroluminescence by Zone Annealing of Spin-Coated and Vacuum-Sublimed Amorphous Films Producing Crystalline Thin Films. *Appl. Phys. Lett.* **2003**, *83*, 5431−5433.
(24) Tripathi, A. K.; Heinrich, M.; Siegrist, T.; Pflaum, J. Growth and Electronic Transport in 9,10-Diphenylanthracene Single Crystals - An Organic Semiconductor of High Electron and Hole Mobility. *Adv. Mater.* **2007**, *19*, 2097−2101.
(25) Liu, C. Y.; Bard, A. J. In-Situ Regrowth and Purification by Zone Melting of Organic Single-Crystal Thin Films Yielding Significantly Enhanced Optoelectronic Properties. *Chem. Mater.* **2000**, *12*, 2353−2362.
(26) Schweicher, G.; Paquay, N.; Amato, C.; Resel, R.; Koini, M.; Talvy, S.; Lemaur, V.; Cornil, J.; Geerts, Y.; Gbabode, G. Toward Single Crystal Thin Films of Terthiophene by Directional Crystallization Using a Thermal Gradient. *Cryst. Growth Des.* **2011**, *11*, 3663−3672.
(27) Zhang, L.; Colella, N. S.; Liu, F.; Trahan, S.; Baral, J. K.; Winter, H. H.; Mannsfeld, S. C. B.; Briseno, A. L. Synthesis, Electronic Structure, Molecular Packing/Morphology Evolution, and Carrier Mobilities of Pure Oligo-/Poly(alkylthiophenes). *J. Am. Chem. Soc.* **2013**, *135*, 844−854.
(28) Zhang, L.; Colella, N. S.; Cherniawski, B. P.; Mannsfeld, S. C. B.; Briseno, A. L. Oligothiophene Semiconductors: Synthesis, Characterization, and Applications for Organic Devices. *ACS Appl. Mater. Interfaces* **2014**, *6*, 5327−5343.
(29) Zhang, L.; Liu, F.; Diao, Y.; Marsh, H. S.; Colella, N. S.; Jayaraman, A.; Russell, T. P.; Mannsfeld, S. C. B.; Briseno, A. L. The Good Host: Formation of Discrete One-Dimensional Fullerene "Channels" in Well-Ordered Poly(2,5-bis(3-alkylthiophen-2-yl)thieno-[3,2-b]thiophene) Oligomers. *J. Am. Chem. Soc.* **2014**, *136*, 18120−18130.
(30) Singh, G.; Yager, K. G.; Smilgies, D. M.; Kulkarni, M. M.; Bucknall, D. G.; Karim, A. Tuning Molecular Relaxation for Vertical Orientation in Cylindrical Block Copolymer Films via Sharp Dynamic Zone Annealing. *Macromolecules* **2012**, *45*, 7107−7117.
(31) Taguchi, K.; Miyaji, H.; Izumi, K.; Hoshino, A.; Miyamoto, Y.; Kokawa, R. Growth Shape of Isotactic Polystyrene Crystals in Thin Films. *Polymer* **2001**, *42*, 7443−7447.
(32) Kyu, T.; Xu, H.; Guo, T.; Wang, G. X. Phase Field Modeling on Polymer Crystallization and Phase Separation in Crystalline Polymer Blends; Isayev, A. I., Ed.; *Encyclopedia of Polymer Blends*; Wiley-VCH Verlag: Weinheim, Chapter 4, 2010; pp 113−151.
(33) Somani, R. H.; Hsiao, B. S.; Nogales, A.; Srinivas, S.; Tsou, A. H.; Sics, I.; Balta-Calleja, F. J.; Ezquerra, T. A. Structure Development during Shear Flow-Induced Crystallization of I-PP: In-Situ Small-Angle X-Ray Scattering Study. *Macromolecules* **2000**, *33*, 9385−9394.
(34) Koutsky, J. A.; Walton, A. G.; Baer, E. Nucleation of Polymer Droplets. *J. Appl. Phys.* **1967**, *38*, 1832−1839.

DOI: 10.1021/acsami.5b06344
ACS Appl. Mater. Interfaces 2015, 7, 23008−23014